International Journal of Remote Sensing
Vol. 26, No. 18, 20 September 2005, 4117–4136

Taylor & Francis
Taylor & Francis Group

Regional accuracy of QuikSCAT gridded winds

G. V. MOSTOVOY*, P. J. FITZPATRICK and Y. LI
GeoResources Institute, ERC, Mississippi State University, PO Box 9652, MS, 39762, USA

(*Received 27 November 2004; in final form 9 March 2005*)

The quality of gridded 00 UTC and 12 UTC QuikSCAT wind speed fields provided by the Florida State University (FSU) and NASA Jet Propulsion Laboratory (JPL) are analysed over the Bay of Bengal during May–August 2001. Additionally, an examination of these fields is performed over the Gulf of Mexico for the May–August period from 2001 to 2003. Both 00 UTC and 12 UTC time almost coincide with QuikSCAT sampling times (twice a day) and correspond to either early morning or late evening local time over these regions. The primary restriction for generating accurate maps with a temporal resolution of 12 hours and less is a lack of adequate sampling. Due to non-uniform spatial-temporal sampling of the scatterometer, interpolation procedures cannot provide proper estimates in data gaps over the regions not covered by a swath. Wind speed autocorrelation coefficients for gridded datasets have been compared with that of original QuikSCAT data and buoy winds. It is shown that the spatial and temporal interpolation used to obtain these datasets results in smoothing of the QuikSCAT wind speeds, reducing their original variance. This smoothing is amplified where substantial diurnal wind variability occurs. A comparison with buoy data shows that FSU and JPL gridded fields are unable to reproduce correctly observed low correlations in wind speed between morning and evening breeze flows and diurnal variability of winds, leading to a reduced difference between 00 UTC and 12 UTC values in comparison with buoys and swath QuikSCAT data. Rather, the FSU and JPL maps describe daily mean fields. Another consequence of the spatial-temporal interpolation is that the winds are distorted at a frequency matching the dominant sampling interval (3–4 days) of QuikSCAT measurements over the Bay of Bengal.

1. Introduction

Data retrieved from the microwave scatterometer SeaWinds (Ku-band active radar) measurements are known as QuikSCAT winds (QuikSCAT 2001). The SeaWinds instrument was launched by NASA in 1999 onboard the QuikSCAT satellite to provide high-resolution surface wind estimates (e.g. Hu and Liu 2002, Katsaros *et al.* 2001). Calibrated against buoy data (e.g. Ebuchi *et al*. 2002), each QuikSCAT point represents a 10-m wind vector averaged over an area of about 25 km × 25 km (QuikSCAT 2001). The high spatial resolution and an ample spatial coverage of QuikSCAT winds, with a nominal swath width extending 900 km to either side of the nadir track, offer a great advantage over conventional measurements. However, sampling limitations in space and time (a revisiting time of QuikSCAT satellite is

*Corresponding author. Email: mostovoi@gri.msstate.edu

International Journal of Remote Sensing
ISSN 0143-1161 print/ISSN 1366-5901 online
http://www.tandf.co.uk/journals
DOI: 10.1080/01431160500165864

about 12 h) and data gaps due to the presence of heavy rain lead to a different spatial density of measurements. This causes difficulties in adequately estimating short-term (from one to several days) and long-term (week, month, or season period) averaged wind fields (e.g. Kelly and Caruso 1990, Zeng and Levy 1995, Bentamy *et al*. 1998, Liu *et al*. 2000, Milliff and Morzel 2001) from scatterometer measurements. A general approach to estimate expected errors resulting from non-uniform sampling for different scatterometers as a function of a map spatial-temporal resolution has been proposed by Schlax *et al*. (2001). They have shown, in particular, that sampling errors (both mean and standard deviation) for QuikSCAT wind speed maps having one-degree and two days resolution are lower than $1\,\mathrm{ms}^{-1}$.

The main goal of this paper is to examine gridded QuikSCAT fields for potential bias (mean difference) and excessive smoothing. Previous quality examinations have mostly been focused on a bulk comparison between swath winds and all available *in situ* measurements (e.g. Freilich and Dunbar 1999, Ebuchi *et al*. 2002), but only few studies examine the accuracy of gridded scatterometer winds (e.g. Bentamy *et al*. 1998, Pickett *et al*. 2003). Due to this reason, we will investigate regional differences and diurnal effects in quality patterns of QuikSCAT map products.

The creation of uniformly gridded wind fields from QuikSCAT measurement swaths is of great interest to atmosphere and ocean modellers. A comprehensive review of the QuikSCAT geophysical applications is presented in Liu (2002). Gridded wind fields with no gaps are easy to use for solving different geophysical tasks. Therefore various types of spatial-temporal interpolation methods are proposed to fill in the spatial gaps of QuikSCAT observations and obtain gridded wind fields (e.g. Zeng and Levy 1995, Liu *et al*. 1998, Pegion *et al*. 2000). Any objective interpolation procedure must preserve, as much as possible, the spatial and temporal wind characteristics/scales resolved by the measurements. It should be noted that for some ocean and wave modelling applications, an accurate representation of spatial gradients in a wind-forcing field is more important than retention of a rather high temporal resolution (one day and less) in the field (Kelly and Caruso 1990). Kelly *et al*. (1999) have shown that for a specified sampling frequency of the instrument a reasonable, physically based accommodation between spatial and temporal resolution of gridded maps can be achieved. Using NASA scatterometer (NSCAT) measurements, they have produced pseudostress maps with 5-day and 2° latitude-longitude resolution over the tropical Pacific Ocean. The interpolation procedure also must not create spurious features like banded structures or induce excessive smoothing and biases. Interpolating procedures converge to an observed data so that results of interpolation produce, in general, lower values at an observed maximum and higher values at a minimum. Therefore smoothing is an attribute of any interpolation/gridding procedure, and in most cases the geophysical application would determine whether smoothing is desired or not. In this study we denote smoothing as excessive only if it results in statistically significant changes in original data. It should be clear that the accuracy of QuikSCAT swath winds is not subjected to question, but for a given sampling frequency of the scatterometer the proper choice of mapping temporal resolution is essential for producing consistent gridded products.

2. Data description

Three QuikSCAT wind datasets collected over the Bay of Bengal (BB) and over the Gulf of Mexico are compared. All datasets correspond to 00 UTC and 12 UTC

(either early morning or late evening), which almost coincide with the times that QuikSCAT passes over these regions. The first dataset is based on swath QuikSCAT wind estimates produced by Remote Sensing Systems (RSS) (QuikSCAT 2001). These surface wind components are spatially interpolated to a $1^\circ \times 1^\circ$ latitude–longitude grid. Interpolation weights are inversely proportional to the distance between observation and grid point. An influence radius of 0.5° is chosen. Only data within ± 45 min of 00 UTC or 12 UTC are used. Originally this dataset was created to validate operational surface wind forecasts over the north Indian Ocean (Fitzpatrick *et al.* 2002) in March–August 2001 using the weather model MM5 (Grell *et al.* 1994). This will be the control dataset because observed winds are only modified by spatial interpolation within the satellite swath, with no temporal or gap filling. Due to the operational nature of the validation fields in this region, the QuikSCAT winds were retrieved using the Ku-2000 model of geophysical function, and from July 2001 with an advanced model (Ku-2001) when it was adopted for wind processing at RSS. Over the Gulf of Mexico, satellite surface winds retrieved with Ku-2001 were used for a whole period of comparison (the May–August period from 2001 to 2003).

The second wind dataset is a gridded field converted from objectively derived surface pseudostresses, which are produced online by the Center for Ocean-Atmospheric Prediction Studies at the Florida State University FSU. The spatial-temporal interpolation is based on the minimization of a cost function with a background wind field representing an 8-day temporal average (Pegion *et al.* 2000). This is a relatively complex and time-consuming procedure due to the global size of the fields and the use of cross validation iteration procedures for determining the weight coefficients. Spatial resolution of this archive is $1^\circ \times 1^\circ$ and fields are available every 6 h. We will call this the FSU dataset.

A simpler algorithm for QuikSCAT wind gridding is used by Liu *et al.* (1998) at NASA's Jet Propulsion Laboratory (JPL). Components of the QuikSCAT wind are objectively interpolated both in time and space to a $0.5^\circ \times 0.5^\circ$ regular grid using the method of successive corrections (Cressman 1959) with weights chosen subjectively. This method was originally used for gridding winds to process data gathered by the NSCAT. A time influence period of 1.5 days and a 5° maximum radius of influence were adopted for interpolation. This global surface winds archive has a 12-h resolution and is available online at near-real time. We will call this the JPL dataset. All comparisons between these datasets were performed on a $1^\circ \times 1^\circ$ latitude–longitude grid and only at points where RSS winds were available. Although other gridded datasets based on QuikSCAT surface winds exist, they are generally produced by blending the scatterometer winds with global analysis/forecast fields. A useful, user-oriented description of available gridded QuikSCAT and NSCAT products has recently been published by Bourassa *et al.* (2003).

Table 1 summarizes the typical accuracy (rms error) of RSS swath data (Wentz *et al.* 2001) and JPL gridded winds (Pickett *et al.* 2003) both for the wind speed and direction. These rms estimates were obtained by the comparison of QuikSCAT datasets with buoy measurements. JPL data demonstrate almost three times less accuracy than RSS winds. Two types of JPL datasets, near-real time and science quality data (values are shown in brackets in table 1), have been validated by Pickett *et al.* (2003). Recently a new RSS gridded product became available online; it represents the swath data mapped to the nearest point of $0.25^\circ \times 0.25^\circ$ regular latitude–longitude grid without any filling of missing values. Unfortunately we

Table 1. Typical rms error between buoys and the QuikSCAT datasets. Estimates for near-real time JPL winds are shown, and the values in brackets stand for science data.

Datasets	Wind speed (ms^{-1})	Wind direction ($^\circ$)	Buoy wind speed (ms^{-1})	Reference
RSS	1.0	15	<20	(Wentz *et al.* 2001)
JPL near shore	3.2 (3.1)	45 (41)	>6	(Pickett *et al.* 2003)
JPL offshore	2.7 (2.5)	42 (41)	>6	(Pickett *et al.* 2003)

could not find direct accuracy references for the FSU QuikSCAT dataset represented by surface pseudostress fields, though some indirect estimates of data quality are available in literature. Studying the Pacific North Equatorial Countercurrent, Yu and Moore (2000) have reported almost the same response of a four-layer ocean model driven by two objective pseudostress fields generated from NSCAT measurements. One was created at FSU using a minimization procedure (Pegion *et al.* 2000), and the other forcing field was generated by an approach intended to preserve the scatterometer resolution within a swath. The method was developed by Kelly *et al.* (1999) for the objective mapping of NSCAT data. The modelling results of Yu and Moore (2000) provide evidence that the objective gridding proposed by Pegion *et al.* (2000) is of a comparable accuracy with other procedures.

The sampling interval of scatterometer winds and their spatial resolution are the most important parameters that control temporal and spatial scales resolved by a spaceborne instrument (Chelton and Schlax 1994). The satellite passes over the region of the BB twice a day, around 00 UTC and 12 UTC, covering the major part of the BB, but not the entire basin. Therefore, QuikSCAT winds are taken irregularly in time with a dominant sampling interval that ranges from one to four days, depending on the location of a sampling region. Figure 1 shows examples of the frequency distribution for RSS winds located within $\pm 1^\circ$ of the tiny squares shown in figure 2. Over the central part of the BB, for example, about one half of the QuikSCAT winds is sampled daily, but the other half is available

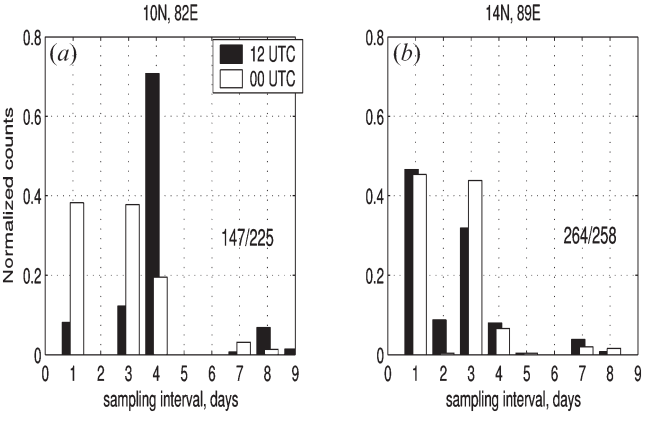

Figure 1. Histograms of sampling interval for QuikSCAT observations (00 UTC and 12 UTC) during May–August 2001 for northern Sri Lanka coast (*a*) and central Bay of Bengal (*b*). Counts in each bin are normalized by total number of observations, depicted by the numerator for 12 UTC and by the denominator for 00 UTC.

only every other day, both at 00 UTC and 12 UTC (see figure 1(*b*)). The region of the NE Sri Lanka coast is under-sampled at 12 UTC, where scatterometer winds are available with a dominant period of four days at 12 UTC (see figure 1(*a*)). The geographical distribution of total wind observations (in counts representing RSS interpolated data at $1^\circ \times 1^\circ$ grid) available over the BB during May–August 2001 is shown in figure 2. The central part of the BB has the greatest data density. The band-like patterns in figure 2 reflect the mean orientation of the satellite track at 00 UTC and 12 UTC. It is clear that highly non-uniform temporal sampling makes the reconstruction of reliable 12 hourly maps over the entire BB impossible.

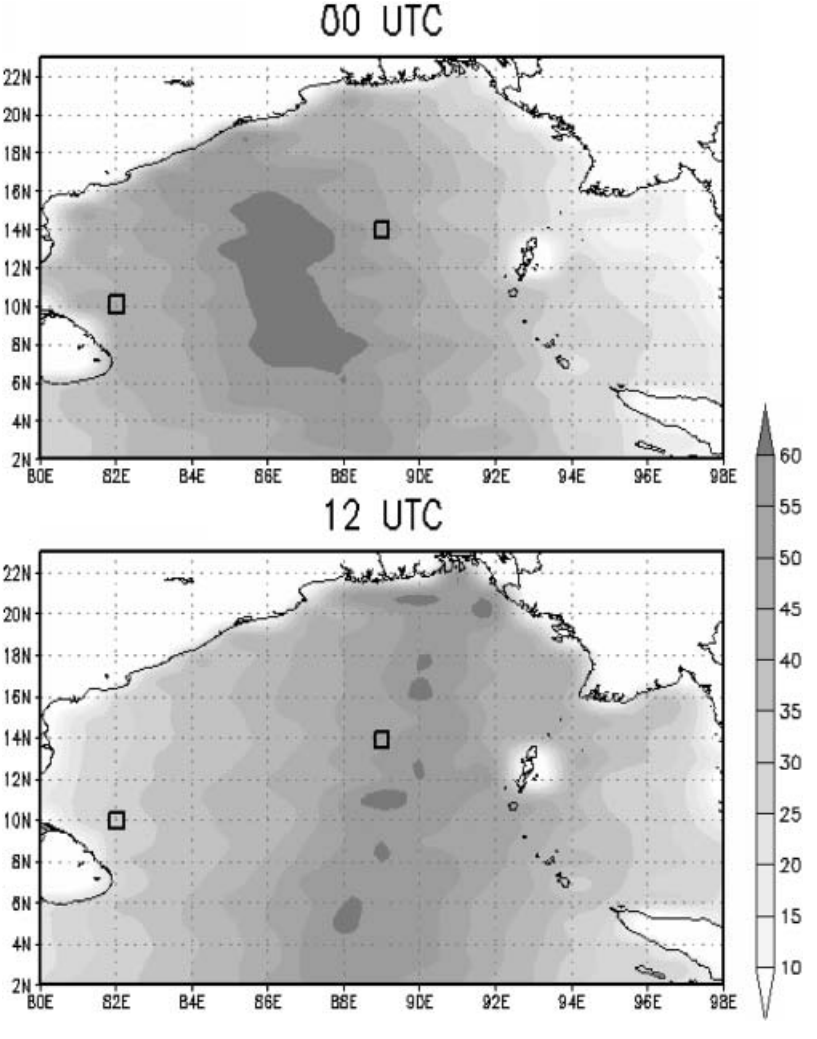

Figure 2. Total number of QuikSCAT observations during May–August 2001 at 00 UTC (upper panel) and 12 UTC (lower panel) on a $1^\circ \times 1^\circ$ latitude–longitude grid. Small squares represent the centre of two regions chosen for detailed comparison of the gridded QuikSCAT fields.

3. Results

3.1 *Comparison over the Bay of Bengal*

It should be noted that a period of May–August chosen for a comparison over the BB is characterized by strong and highly persistent south-westerly surface winds. A directional steadiness measured as a ratio between a vector mean and a scalar mean wind exceeds 0.9 (Hastenrath and Lamb 1979) over the open BB. This atmospheric flow reflects an exceptional planetary-scale phenomenon—the Indian monsoon, which has occasional 6–10 day spans of low winds known as breaks in the monsoon.

Before comparing the QuikSCAT gridded products, important regional features of wind speed variability as revealed by the RSS dataset require discussion. Because moored observations over the BB are available only for relatively short periods during special observational experiments (e.g. Bhat 2001), we will consider RSS as a control dataset. Time series of RSS wind speed are shown in figure 3 at the two box points, with the location over the BB depicted in figure 2. North-east Sri Lanka exhibits noticeable diurnal variability in wind speed (figure 3(*b*)). The wind speed at 12 UTC (6 p.m. local time) is consistently lower than the speed at 00 UTC (6 a.m. local time). Further evidence of this diurnal variability is shown through scatterplots of wind speed (figure 4(*a*)), which do not reveal a correlation between 00 UTC and 12 UTC winds behind Sri Lanka. The correlation coefficient (R_{12}) is 0.293; whereas, wind sets lagged by 24 h have a stronger correlation of R_{24}=0.784.

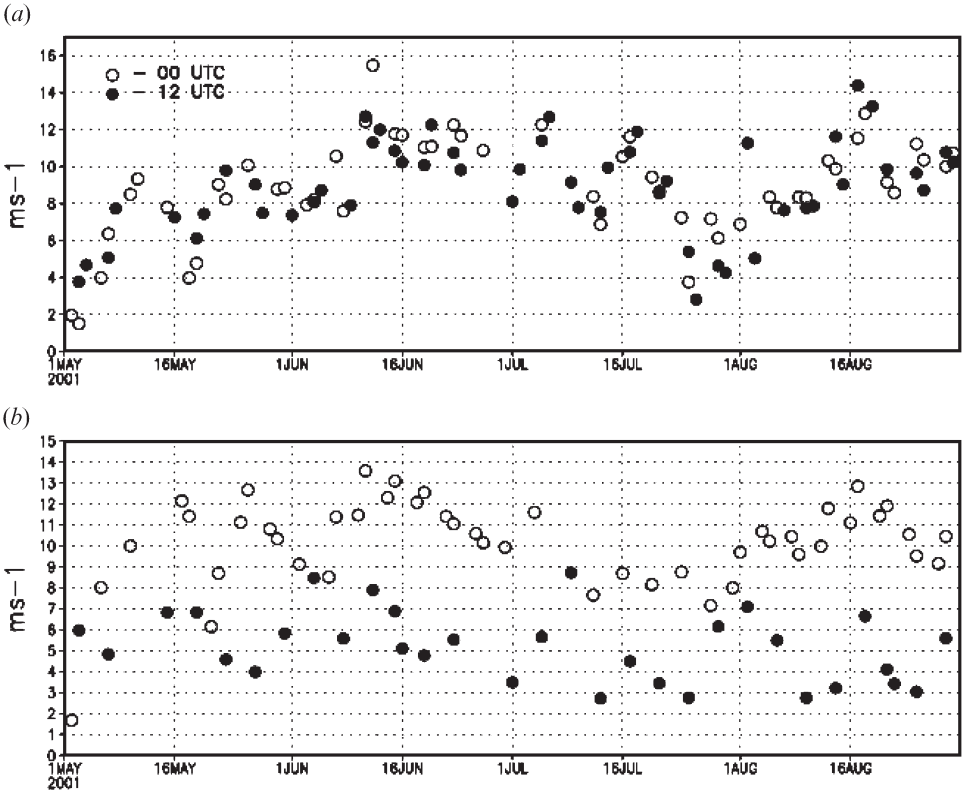

Figure 3. Examples of QuikSCAT wind speed temporal variability on $1^\circ \times 1^\circ$ latitude–longitude grid (RSS dataset) (*a*) for open BB region, and (*b*) for coastal zone.

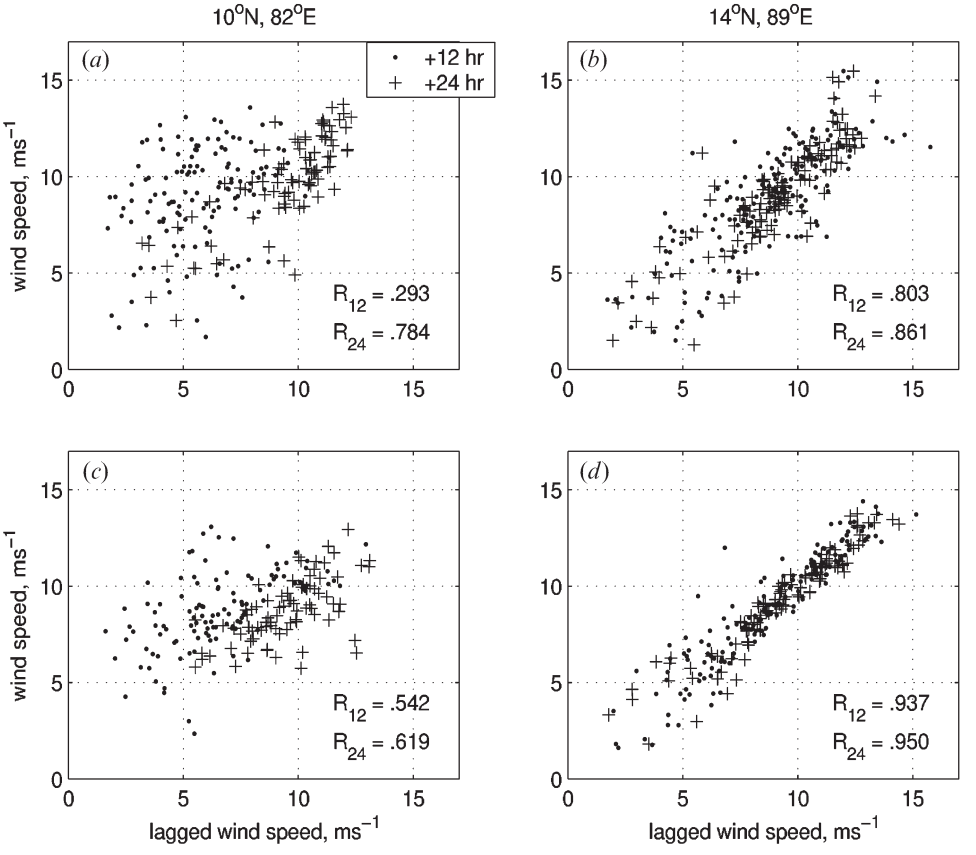

Figure 4. Scatterplots of the QuikSCAT wind speed for 12-h and 24-h time lag for Sri Lanka (*a, c*) and the central BB (*b, d*). R_{12} and R_{24} are correlation coefficients of the wind speed for 12-h and 24-h lags. The top (*a, b*) figures are for raw QuikSCAT data (RSS), and the bottom figures (*c, d*) are for gridded JPL data. Note a reduction of variance in JPL winds in the open ocean region (*d*) as compared with RSS values (*b*) due to the smoothing effect of temporal interpolation.

The weak correlation between 00 UTC and 12 UTC winds is due to the diurnal wind cycle in north-east Sri Lanka. During the evening hours (12 UTC) the sea breeze over the northern coast of Sri Lanka tends to blow against the south-westerly monsoon flow, thus leading to a weaker wind. This difference between 00 UTC and 12 UTC winds is not manifested over the central BB (figure 3(*a*)). Strong correlations exist both for 12-h (R_{12}=0.803) and 24-h (R_{24}=0.861) lags, as shown in figure 4(*b*). The sampling area chosen for the analysis over the NE coast of Sri Lanka was centred at 10° N and 82° E, including the four nearest grid points within $\pm 1°$ latitude-longitude range. For such a configuration of the sample area, the nearest point of the grid was located about 100 km from the coast and the furthest at about 300 km. Note that every RSS grid point value is a result of bilinear interpolation of swath winds with an influence radius of 0.5°. Performing observational and theoretical studies of breeze circulation over the Gulf of Mexico, Nielsen-Gammon (2001) has reported an unusually large seaward extent, up to 400 km of the land/sea breeze. This large horizontal scale is supported by a simple linear theory of the subtropical breeze, which predicts an increase in this scale towards the equator.

The same analysis is now performed on the gridded datasets. A smoothing effect due to the temporal interpolation of winds is evident in figures 4(*c*) and (*d*) for all regions in the JPL dataset, with larger effects in north-east Sri Lanka. FSU fields also exhibit similar smoothing features (not shown). JPL winds generally show lower variance and higher correlation for 12-h time lags. A major change of R_{12} from 0.293 (RSS winds) to 0.542 (JPL winds) is observed over north-east Sri Lanka where the observation density is relatively low (figure 2). Spatial distributions of R_{12} and R_{24} also show this difference off Sri Lanka (figure 5), as well as generally higher correlations for JPL data compared to RSS data for all locations. We can conclude, therefore, that the spatial-temporal interpolation procedures used to create gridded QuikSCAT winds in the BB alter the original properties of QuikSCAT winds, due to smoothing.

To further quantify the impact of diurnal variability on the quality of gridded fields, suppose that temporal interpolation procedures do not take into account the weak relationship between current and 12-h old winds in north-east Sri Lanka, so the weight function is monotonically decaying with time. JPL and FSU winds interpolated with such weights would be generally underestimated at 00 UTC and overestimated at 12 UTC compared with the RSS reference values. Wind speed

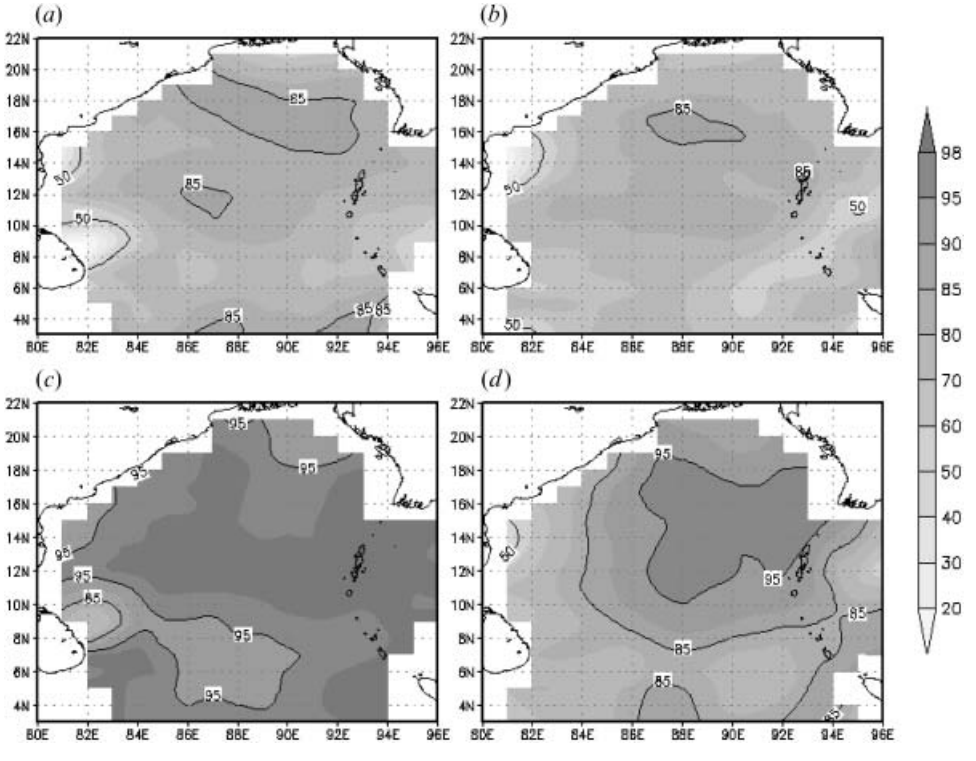

Figure 5. Geographical distribution of autocorrelation coefficients for the QuikSCAT wind speed at 12-h (*a, c*) and 24-h (*b, d*) time lags for RSS (*a, b*) and JPL (*c, d*) datasets. Correlation coefficients are multiplied by 100. Values of R_{12} and R_{24} are elevated for the JPL dataset compared with RSS winds. Note that low R_{12} values (<0.5) for RSS winds (*a*) are concentrated in north-east Sri Lanka. This implies that wind speed interpolation from 00 UTC and 12 UTC and vice versa is not statistically justified in regions subject to diurnal wind variations, such as Sri Lanka.

differences (RSS-JPL) and (RSS-FSU) are used here as a measure of this bias. The difference should be mostly positive at 00 UTC and mostly negative at 12 UTC if the above assumptions about the weight function are valid.

Indeed, histograms of these differences for north-east Sri Lanka (figures 6(*a*) and (*c*)) show a tendency for positive values prevailing at 00 UTC and for negative values at 12 UTC. Note that this systematic shift between 00 UTC and 12 UTC in the distribution is not observed over the central BB (figures 6(*b*) and (*d*)). This tendency is also manifested in JPL and FSU long-term mean fields for north-east Sri Lanka, which show negative bias at 12 UTC (figures 7(*a*) and (*b*)) and positive bias at 00 UTC (figures 7(*c*) and (*d*)). The magnitude of this bias exceeds $2\,\mathrm{ms}^{-1}$ at 00 UTC and 12 UTC. Patterns of these fields do not appear to be spatially random.

Figure 7 also shows a mean vector difference (vector bias) between RSS and JPL datasets and between RSS and FSU winds. The vector bias fields also demonstrate consistent regional patterns both at 00 UTC and 12 UTC, indicating a direct influence of land-sea breeze on JPL and FSU gridded winds. The strong north-easterly vector bias is observed at 12 UTC (figures 7(*a*) and (*b*)), and south-westerly vector bias is dominated at 00 UTC (figures 7(*c*) and (*d*)) over north-east Sri Lanka. The above differences between RSS and other gridded mean values of the wind speed at 12 UTC have proven to be significant at 99% for RSS/FSU pair and at 95% level for RSS/JPL pair within the region behind Sri Lanka. The grid cell centred at

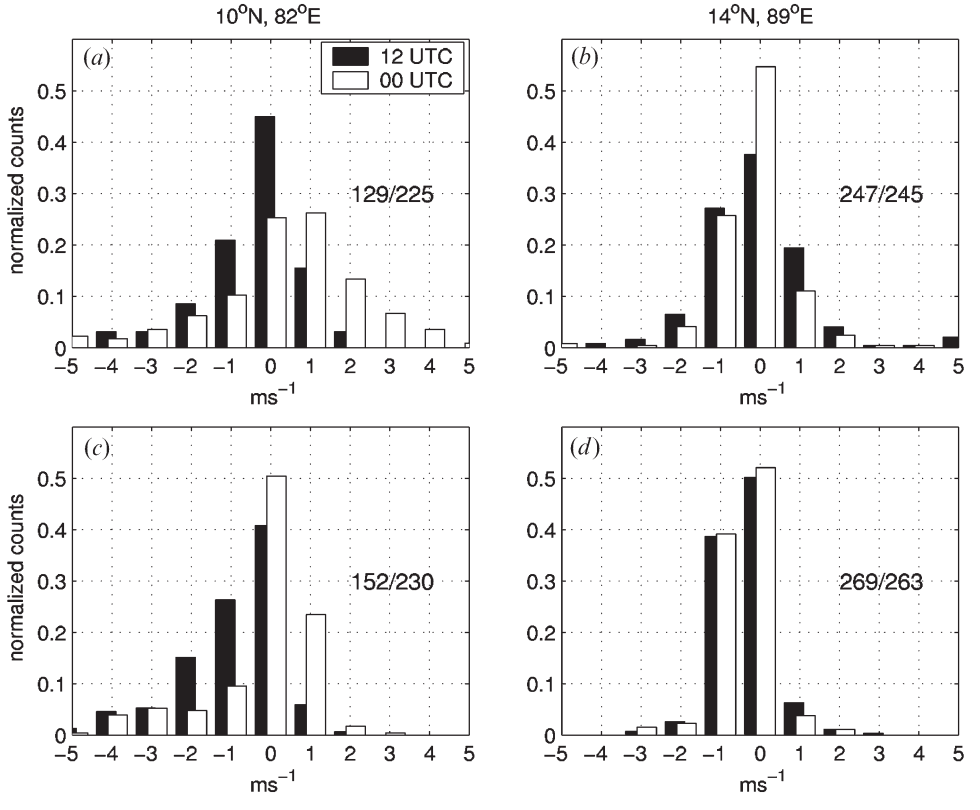

Figure 6. Histograms of wind speed difference between RSS and JPL datasets (*a, b*), and between RSS and FSU datasets (*c, d*). Counts in each bin are normalized by total number of observations, shown by numerator for 12 UTC and by denominator for 00 UTC.

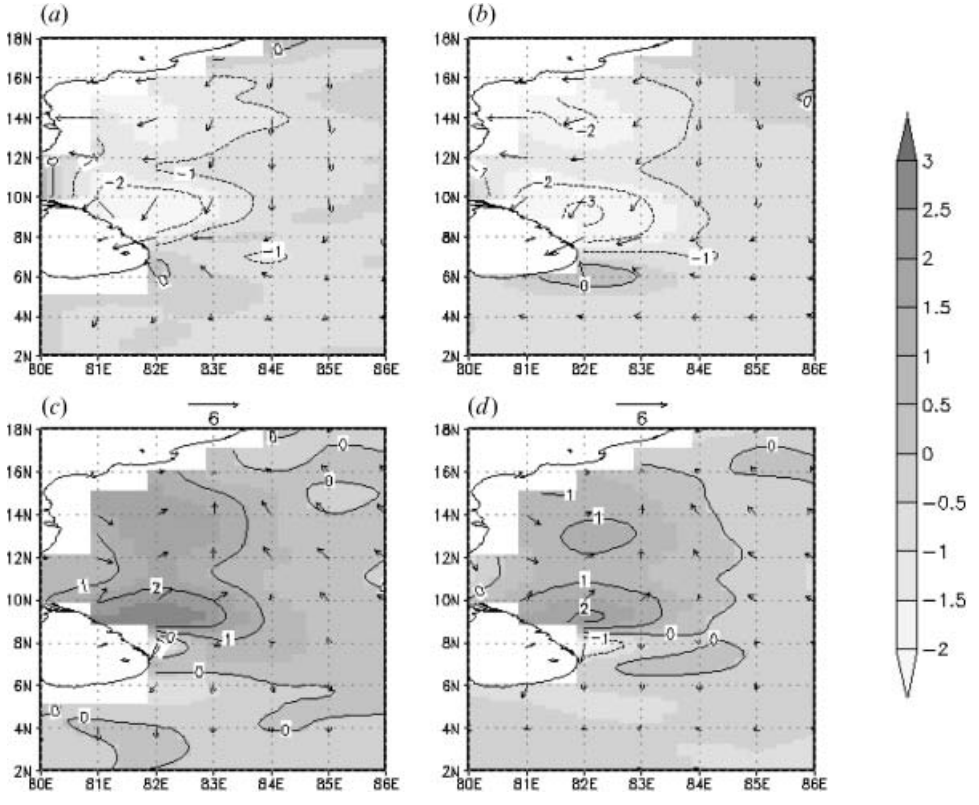

Figure 7. Vector and magnitude differences (both in ms^{-1}) off north-east Sri Lanka averaged from May to August 2001 between RSS and JPL winds (*a*); and between RSS and FSU winds (*b*) for 12 UTC. (*c*) and (*d*) are as (*a*) and (*b*), but for 00 UTC.

10° N and 82° E (see figure 2 for its location) and four adjacent cells are used for the mean wind speed estimates for the *t*-test (the number of degrees of freedom is 450). The positive bias in the morning (00 UTC) has proven to be insignificant at 90% level. A similar *t*-test has been performed over the open BB area (see figure 2 for its location) having 500 degrees of freedom. It shows that, for both 00 UTC and 12 UTC, there is no statistically significant difference in the mean wind speed between RSS and other gridded datasets. Corresponding *t*-values are well below the 90% level of significance.

Another consequence of the interpolation procedures used to generate gridded scatterometer fields is that winds are distorted at a frequency associated with the dominant sampling interval of QuikSCAT measurements. Figure 8 shows an autocorrelation function of the FSU winds over north-east Sri Lanka at 12 UTC and 00 UTC. The FSU dataset reveals spurious 4-day periodicity related to the dominant 4-day sampling interval of QuikSCAT observations at 12 UTC (see figure 1(*a*)). This is a common drawback of satellite gridded products, which has been recognized by the community (e.g. Zeng and Levy 1995). Performing a general analysis of potential scatterometer instrument sampling errors, Schlax *et al.* (2001) have predicted the 4-day periodicity in the amplitude of an expected sampling relative error for QuikSCAT winds (see figure 15(*d*) relating to 25N from their paper), although they consider a full daily coverage without a distinction between revisiting times.

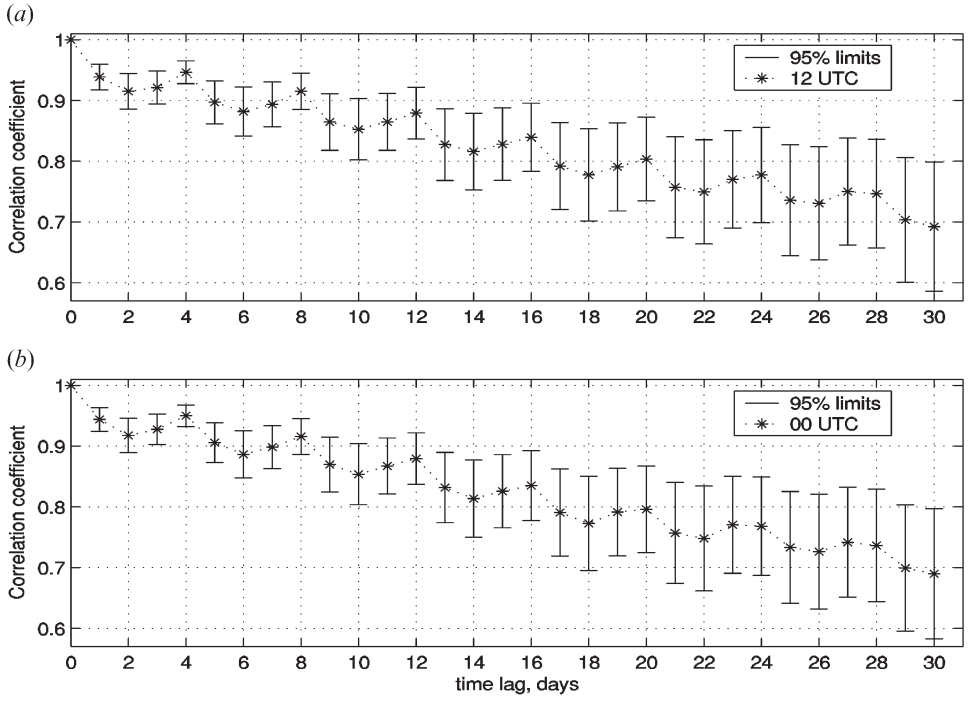

Figure 8. Autocorrelation function of the FSU gridded wind speed datasets for 12 UTC (*a*) and 00 UTC (*b*) at 10° N, 82° E over the time period 1 May–31 August 2001. Confidence limits (95%) are shown as error bars. Both datasets show spurious 4-day periodicity related to the dominant 4-day sampling interval of QuikSCAT observations at 12 UTC (see figure 1(*a*)). Note that 12 UTC winds also generate 4-day periodicity in 00 UTC time series due to the interpolation procedure.

However, previous studies have demonstrated that QuikSCAT gridded winds provide more accurate estimates of the amplitude of surface wind oscillations with a typical periodicity exceeding 10-days, than with conventionally observed winds. For example, Grodsky and Carton (2001) have compared spectra of zonal wind from NCEP/NCAR atmospheric reanalysis fields (Kalnay *et al*. 1996) with that produced by JPL data. Their results, both for reanalysis and JPL fields, have showed quasi-biweekly and 3–5-day (African Waves) oscillations in zonal winds associated with the summer West African Monsoon. The amplitude of the quasi-biweekly oscillations in the JPL data has proven to be nearly twice stronger than in the reanalysis fields, implying that the scatterometer retains the intensity of observed winds better than the reanalysis. Conversely, the amplitude of the 3–5-day disturbances was nearly the same for these two datasets. These facts reflect a general tendency for deterioration of gridded QuikSCAT wind quality with migration from a low- to a high-frequency spectrum interval related to atmospheric disturbances having typical periods of less than 4 days. Because this 4-day threshold is also close to the 3–4-day dominant sampling interval of QuikSCAT winds, causing a spurious periodicity in gridded fields, one can conclude that the deterioration of the high-frequency spectrum of gridded winds is related to a temporal sampling limit of QuikSCAT measurements.

Recent publications (Parés-Sierra *et al*. 2003, Bordoni *et al*. 2004) also demonstrate the usefulness of JPL QuikSCAT gridded winds for analysing typical

seasonal patterns of low-level atmospheric circulations at a regional scale (over the Gulf of California). Unlike our examination, which focused on diurnal variability of winds, these studies have used daily averaged fields. Analysing daily JPL winds over the Gulf of California, Parés-Sierra *et al.* (2003) and Marinone *et al.* (2004) have provided examples of misleading results caused by non-adequate tuning of the interpolation procedure over areas under-sampled by the scatterometer.

3.2 *Comparison over the Gulf of Mexico*

A similar comparison has been performed over the Gulf of Mexico. The same datasets (RSS, FSU and JPL) of QuikSCAT winds are used to demonstrate that results of comparison obtained over the BB can be also observed in other oceanic regions. An analysis covers the same months from May to August, but it is extended for the 3-year time period from 2001 to 2003. Additionally the FSU, JPL and RSS datasets are compared against *in situ* wind speed measurements from US National Data Buoy Center ocean buoys. Quality controlled observations from 11 moored buoys are used for comparison. Their locations over the northern part of the Gulf of Mexico are shown in figure 9. The QuikSCAT data provide an estimate of the 10-m neutral equivalent wind (Verschell *et al.* 1999). Therefore, all wind speed buoy observations have been adjusted to heights of 10 m, using a power-law profile with an exponent equal to 0.1. The effects of stability correction have little impact on the results of comparison (see Appendix).

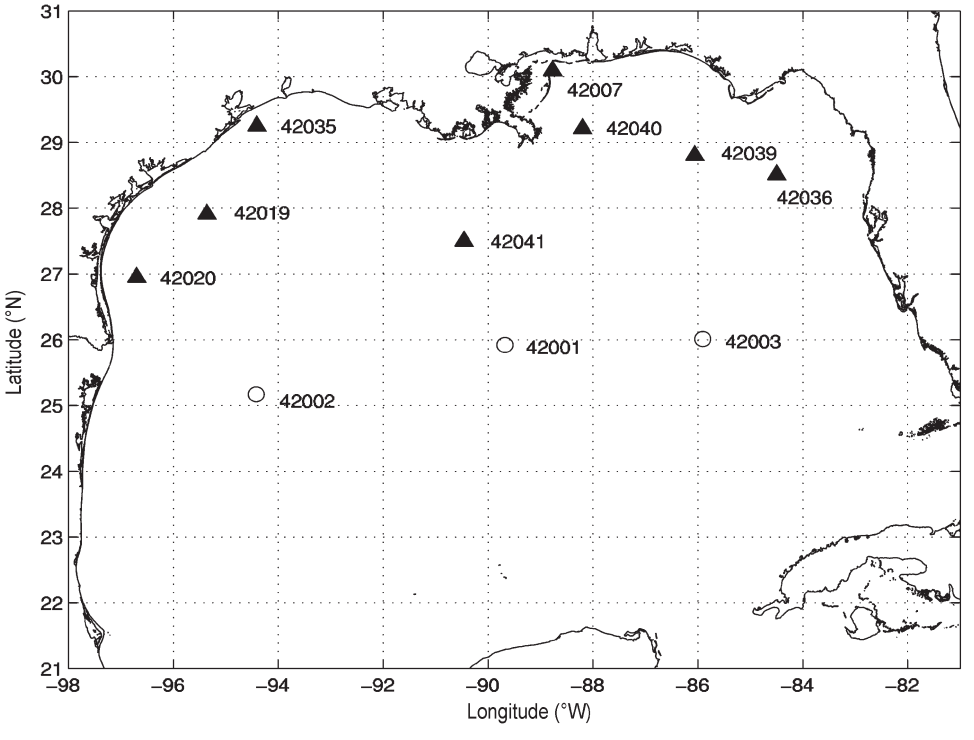

Figure 9. Locations of the US National Data Buoy Center buoys used in this study. Triangles indicate which buoy winds are adjusted to 10-m height. Figures stand for a buoy number.

Freilich and Dunbar (1999) used all the buoys shown in figure 9, except for 42007 and 42041, for the verification of the NSCAT wind vectors. They demonstrated that observations from these buoys are meteorologically representative, having significant vector correlations with scatterometer winds. This means that synoptic scale flow measured from satellite is not distorted by local influences.

Surface airflow in the north-west part of the Gulf of Mexico is dominated by south-easterly winds during the summer. In this region they are more directionally persistent than in other parts of the Gulf of Mexico. Diurnal variations in the wind direction are modulated by a land-sea breeze close to a coastline. Because this persistency in the wind direction makes the diurnal variability more pronounced, we consider this region of the Gulf of Mexico. In general there is a substantial bias of about 30° between morning (12 UTC or 6 a.m. local time) and evening flow (00 UTC or 6 p.m. local time) in this area. This systematic shift in the direction between morning and evening air currents is plainly supported by histograms of the observed wind direction at 12 UTC and 00 UTC (figures not shown). This feature is observed most clearly at buoy 42020 where the coastline is nearly perpendicular to the u-component of the wind, which is positive when directed to the east. At this location the u-component or a zonal wind is oriented along the land–sea breeze flow. Therefore in the morning the breeze current is directed against the u-component (of the south-easterly main surface flow), leading to its lowering. In contrast, during the evening the u-component increases because its direction coincides with that of the breeze flow. This diurnal cycle in the u-component makes the direction of resultant winds more easterly in the evening and more southerly in the morning.

Due to this diurnal variation, the observed zonal wind at buoy 42020 shows zero correlation coefficient between 00 UTC and 12 UTC values ($R_{12}=-0.037$). At the same time, the correlation coefficient is dramatically higher for 24-h lag ($R_{24}=0.600$), as illustrated by zonal wind scatterplots in figure 10(*a*). A similar relationship between R_{12} and R_{24} values of the zonal wind series is also manifested for other buoys (42019 and 42035) in this part of the Gulf of Mexico and for RSS dataset as well (figure 10(*d*)). To compare the gridded winds with buoy observations, grid point values nearest to the buoy location are selected. Figures 10(*b*) and (*c*) show scatterplots and correlation coefficients of the zonal wind with 12-h and 24-h lags for FSU and JPL datasets. As shown in figures 10(*b*) and (*c*), the zonal wind exhibits much stronger correlations between 00 UTC and 12 UTC series for FSU and JPL when compared with that of the observed and RSS zonal wind (figures 10(*a*) and (*d*)). The correlation coefficient R_{12} increases to 0.726 and to 0.649 for FSU and JPL series respectively. As in the case of the BB, this apparent disagreement in R_{12} values calculated from observations and from gridded QuikSCAT datasets is a direct result of the time interpolation with monotonically decreasing weights. This feature is limited to regions with substantial diurnal variability of winds. Unlike the above changes in R_{12} values, there are no feasible variations in the correlation coefficient with a 24-h lag for the zonal wind between buoy, FSU, JPL, and RSS data. Naturally, temporal sampling deficiency is a primary reason for the poor quality of the 12-h wind maps revealed in overestimates of R_{12}. But the application of a properly adjusted interpolation scheme is also important. Using non-monotonic weights matching actual low correlations for 12-h lag, one can improve current interpolation results over this region. To achieve a better accuracy of wind maps, a more versatile interpolator taking into account observed statistics in coastal regions along with a wind field over the land should

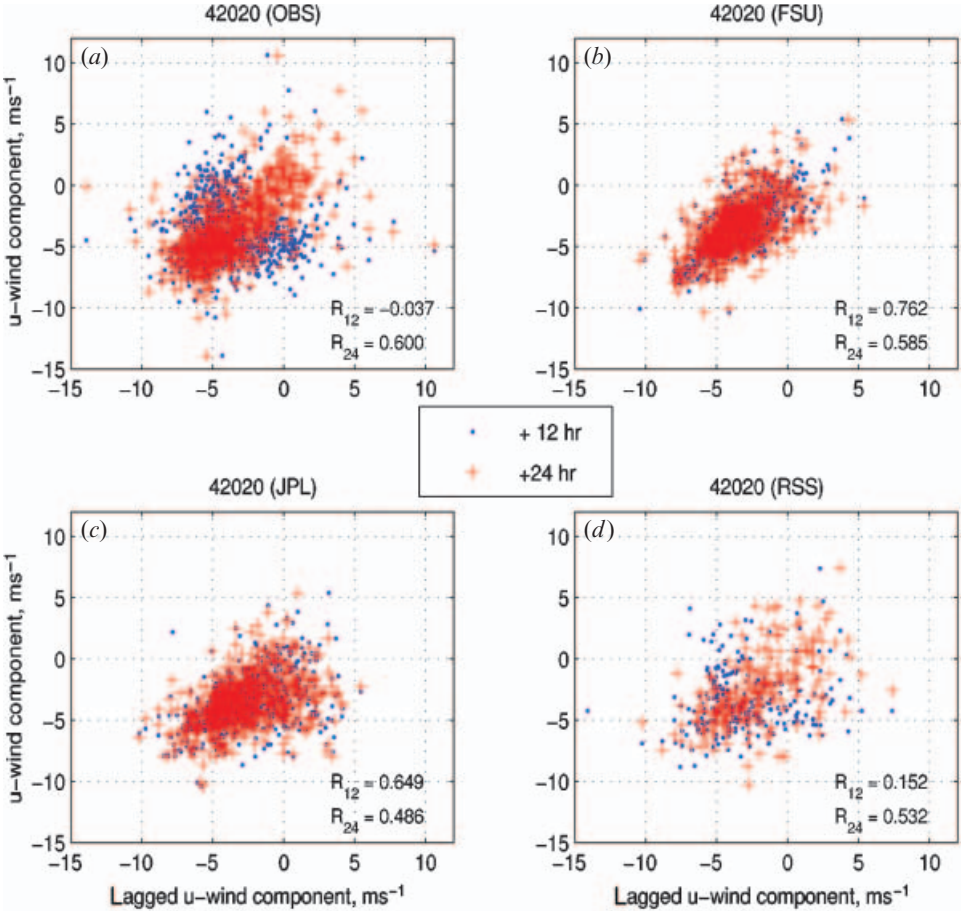

Figure 10. Scatterplots of zonal winds for ± 12-h and ± 24-h time lags for 42020 buoy. The frame (*a*) is for buoy observations, (*b*) is for FSU, (*c*) is for JPL, and (*d*) is for RSS zonal winds. R_{12} and R_{24} are correlation coefficients of the zonal wind speed for 12-h and 24-h lags. Note a substantial reduction of variance in FSU and JPL gridded data as compared with observation and RSS values.

probably be used, as suggested by Zeng and Levy (1995). Kelly and Caruso (1990) reported similar difficulties in adequate specification of statistical interpolation parameters (variances and decorrelation scales) for coastal regions.

Another way of describing the smoothing effect of temporal interpolation is shown in figure 11, where histograms of the difference between buoy and QuikSCAT (JPL, FSU, and RSS) zonal wind are plotted for buoy 42020. The zonal wind for both JPL and FSU is biased relatively low at 00 UTC and relatively high at 12 UTC as compared to the buoy data. There are no such biases in RSS zonal winds; therefore, distributions of the buoy-RSS difference at 00 UTC and 12 UTC are almost identical in shape and nearly normal (see figure 11(*c*)). These peculiarities are similar to those estimated over the BB in north-east Sri-Lanka (see figures 6(*a*) and (*b*)), indicating that the monotonically decreasing time–weight function does not reproduce an observed correlation lowering correctly at the 12-h lag in comparison with that at the 24-h lag. A *t*-test with 720 degrees of freedom is also performed to evaluate the statistical significance of zonal wind differences for

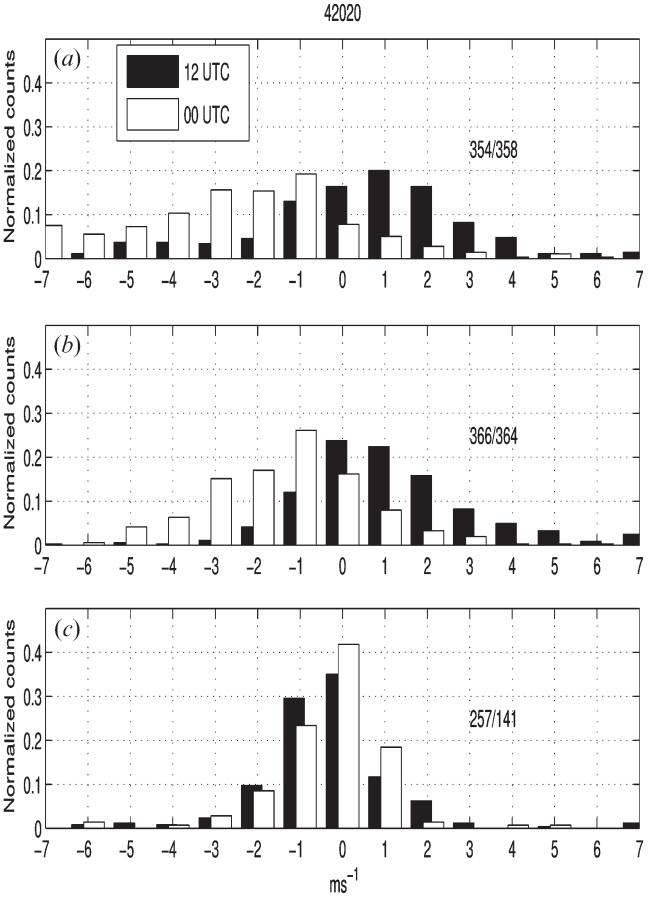

Figure 11. Histograms of buoy-JPL (*a*), of buoy-FSU (*b*), and of buoy-RSS (*c*) zonal wind difference for 42020 buoy. Counts in each bin are normalized by total number of observations, shown by numerator for 12 UTC and by denominator for 00 UTC.

JPL and FSU datasets over the coastal zone of the Gulf of Mexico. The test shows that the mean values of zonal wind between the 42020 buoy and QuikSCAT gridded winds are significantly different both for 00 UTC and 12 UTC at the 99% level, except for a JPL sample at 12 UTC which has the 95% significance level. A similar *t*-test for the buoy/RSS pair has revealed that there is no statistically significant difference in mean values between the 42020 buoy and RSS zonal winds. Estimated absolute *t*-values (t) have proven to be much lower than those for the 90% level of significance for both at 00 UTC ($t=-1.723$) and 12 UTC ($t=-1.051$). Likewise in the open part of BB (see figures 6(*c*) and (*d*)), there is no such separation in zonal wind difference distributions between 00 UTC and 12 UTC both for buoy-JPL and buoy-FSU over central regions of the Gulf of Mexico. Unlike the coastal zone, there are no statistically significant changes in the mean zonal wind between the 42001 buoy (the central Gulf of Mexico) and gridded datasets. Corresponding *t*-values have proven to be less than that for the 90% level of significance.

The smoothing effect of the temporal interpolation is also apparent as an overall reduction of the scatter in FSU and JPL wind speed datasets in comparison with observations and RSS winds. Correlation coefficients between 00 UTC and 12 UTC

wind speeds have been calculated to quantify this reduction in the data points scatter. They are plotted in figure 12 along with 95% confidence limits for all the buoys used in this study. Correlations coefficients for FSU and JPL datasets are significantly higher than for observations and RSS winds at all buoys except for 42007, indicating an alternation of original statistical properties by FSU and JPL interpolation.

Although gridded QuikSCAT products are useful for the analysis of quasi-biweekly wind oscillations (Grodsky and Carton 2001), this study has shown that FSU and JPL gridded datasets failed to reproduce adequately diurnal variability of winds, leading to a reduced difference between 00 UTC and 12 UTC values in comparison with observations and RSS data. Rather, the FSU and JPL gridded products describe daily mean fields.

Potential implications of these features in FSU and JPL maps for ocean and wave modelling studies are limited to near shore zones (up to 300 km from the coast) over the regions with a substantial diurnal variability of winds. It is a geophysical/ocean model that controls by itself the necessary temporal and spatial resolution of input forcing fields. If a typical time scale of one day or longer is required for these fields, then FSU and JPL daily-averaged, $0.5^\circ \times 0.5^\circ$ maps can provide accurate input. Although forcing with high resolution of 50 km and more is essential for an adequate simulation of ocean mesoscale features like fronts and eddies (e.g. Kelly and Caruso 1990), a high frequency input (6-hourly fields) is also important for an explicit modelling of near-inertial frequency, a part of the wave spectrum associated with a wind forcing (e.g. Fox *et al.* 2000, Zavala-Hidalgo *et al.* 2003). In the latter case, use of FSU maps over near shore regions with 6-h resolution might cause problems due to an excessive smoothing of diurnal variability in these maps.

4. Conclusions

It is demonstrated that the FSU and JPL procedures used to generate 00 UTC and 12 UTC gridded winds with $0.5^\circ \times 0.5^\circ$ resolution from QuikSCAT measurements result in smoothing of the original fields over the Bay of Bengal and over the Gulf of Mexico. Both 00 UTC and 12 UTC time almost coincide with the QuikSCAT sampling times (twice a day) and correspond to either early morning or late evening local time over these regions. Synthesis of accurate wind maps with 12-hour and

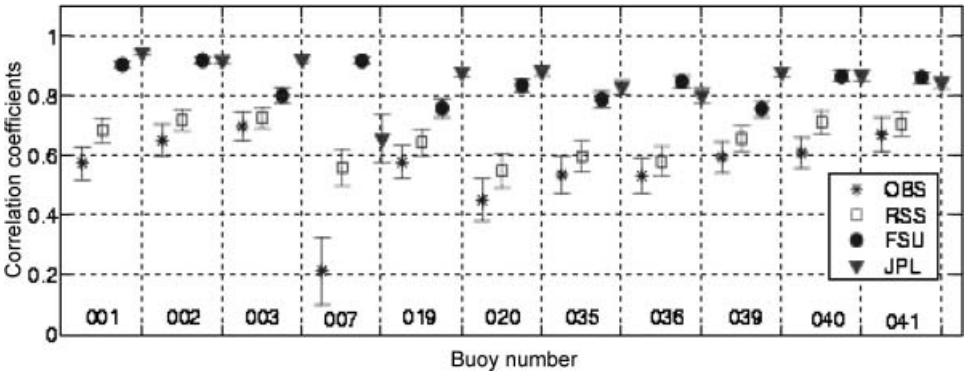

Figure 12. Correlation coefficients between 00 UTC and 12 UTC wind speed for different datasets. Abscissa corresponds to the buoy number (region prefix 42 is omitted). Error bars stand for 95% confidence limits.

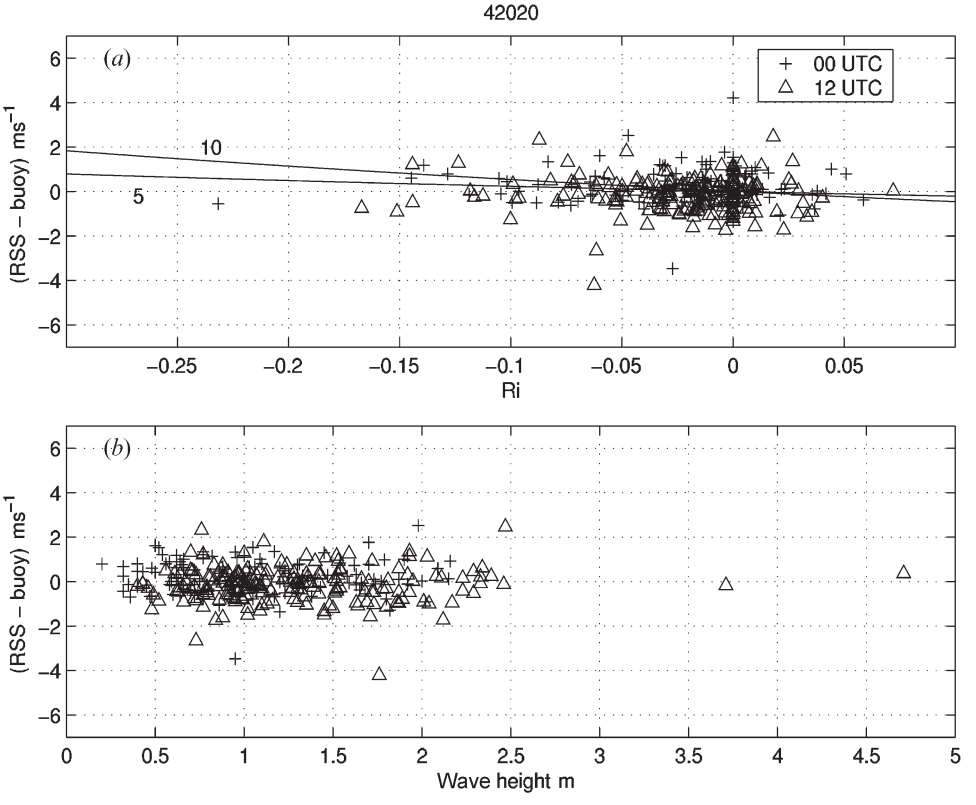

Figure 13. Dependence of wind speed residuals (RSS–buoy) on Ri number (*a*) and on wave height (*b*) for 42020 buoy. Lines denoted by numbers 5 and 10 indicate an expected relationship between a stratification surplus to the wind residuals and Ri for the buoy wind speed 5 ms^{-1} and 10 ms^{-1}.

higher temporal resolution is mainly limited by a deficiency in adequate sampling. Due to the non-uniform spatial-temporal sampling of the scatterometer, interpolation procedures cannot provide proper estimates in data gaps over the regions not covered by a swath. The effect of smoothing can be amplified over the coastal regions where diurnal wind variability is important, such as north-east Sri Lanka, leading to wind speed biases exceeding 2 ms^{-1} in magnitude. A comparison with both buoy and RSS data shows that FSU and JPL interpolators are unable to mimic observed low correlations in wind speed between morning and evening breeze flows. As a result, there is a tendency for underestimation of the wind speed in the evening and for overestimation in the morning hours, causing an overall reduced difference between 00 UTC and 12 UTC values in comparison with buoys and swath QuikSCAT data. Rather, the FSU and JPL maps describe daily mean fields. An interpolation procedure that accounts for actual statistical properties of QuikSCAT winds can reduce this deficiency. Although winds over the Gulf of Mexico are not as strong and persistent as winds over the Bay of Bengal, the diurnal patterns of bias distribution for the gridded winds are similar, indicating that these properties in QuikSCAT gridded fields are expected to be observed in other oceanic regions. Users of gridded QuikSCAT datasets should be aware of these potential biases and assess whether this will significantly impact their research objectives.

Acknowledgements

Encouragement by Dr Roger King and financial support from the GeoResources Institute are highly appreciated. The authors greatly acknowledge consultations provided by Deborah Smith, Remote Sensing Systems (Santa Rosa, CA), on reading and understanding the QuikSCAT datasets. The JPL winds are obtained from NASA/NOAA courtesy of W. Timothy Liu and Wenqing Tang. The authors greatly appreciate the efforts of Mark Bourassa, Center for Ocean-Atmospheric Prediction Studies at FSU, for maintaining the COAPS scatterometer web page. We are grateful to Valentine Anantharaj of MSU for making valuable comments on this manuscript. We are also grateful to anonymous reviewers for making useful suggestions that improved the text significantly.

References

Bentamy, A., Grima, N. and Quilfen, Y., 1998, Validation of the gridded weekly and monthly wind fields calculated from ERS-1 scatterometer wind observations. *The Global Atmosphere and Ocean System*, **6**, pp. 373–396.

Bhat, G.S., 2001, Near surface atmospheric characteristics over the North Bay of Bengal during the Indian summer monsoon. *Geophysical Research Letters*, **28**, pp. 987–990.

Bordoni, S., Ciesielski, P.E., Johnson, R.H., McNoldy, B.D. and Stevens, B., 2004, The low-level circulation of the North American Monsoon as revealed by QuikSCAT. *Geophysical Research Letters*, **31**, L10109, doi: 10.1029/2004GL020009.

Bourassa, M.A., Legler, D.M. and O'Brien, J.J., 2003, Scatterometry data sets: High quality winds over water. In *Advances in the Applications of Marine Climatology: The Dynamic Part of the WMO Guide to the Applications of Marine Climatology*, WMO/TD-1081, pp. 159–174 (Geneva, Switzerland: World Meteorological Organization).

Chelton, D.B. and Schax, M.G., 1994, The resolution capability of an irregularly sampled dataset: with application to GeoSat altimeter data. *Journal of Atmospheric and Oceanic Technology*, **11**, pp. 534–550.

Cressman, G.P., 1959, An operational objective analysis system. *Monthly Weather Review*, **87**, pp. 367–374.

Ebuchi, N., Graber, H.C. and Caruso, M.J., 2002, Evaluation of wind vectors observed by QuikSCAT/SeaWinds using ocean buoy data. *Journal of Atmospheric and Oceanic Technology*, **19**, pp. 2049–2062.

Fitzpatrick, P.J., Mostovoi, G.V. and Li, Y., 2002, Validation and comparison of a mesoscale model and NOGAPS in the Bay of Bengal and Arabian Sea for March–August 2001. Technical Report, available from Mississippi State University ERC, 88 pp.

Fox, A.D., Haines, K. and de Cuevas B.A., 2000, Modeling internal waves with a Global Ocean model. *International WOCE Newsletters*, **39**, pp. 27–30.

Freilich, M.H. and Dunbar, R.S., 1999, The accuracy of the NSCAT-1 vector winds: Comparisons with National Data Buoy Center buoys. *Journal of Geophysical Research*, **104**, pp. 11231–11246.

Grell, G., Dudhia, J. and Stauffer, D.R., 1994, A description of the Fifth-Generation Penn State/NCAR Mesoscale Model (MM5). *NCAR/TN398+STR*, 138 pp.

Grodsky, S.A. and Carton, J.A., 2001, Coupled land/atmosphere interactions in the West African Monsoon. *Geophysical Research Letters*, **28**, pp. 1503–1504.

Hastenrath, S. and Lamb, P.J., 1979, *Climatic Atlas of the Indian Ocean. Part I: Surface climate and atmospheric circulation* (Wisconsin: University of Wisconsin Press).

Hu, H. and Liu, W.T., 2002, QuikSCAT reveals the surface circulation of the Catalina Eddy. *Geophysical Research Letters*, **29**, p. 1821.

Kalnay, E.M., Kanamitsu, M., Kistler, R., Collins, W., Deaven, D., Gandin, L., Iredell, M., Saha, S., White, G., Woollen, J., Zhu, Y., Chelliah, M., Ebisuzaki, W., Higgins, W., Jahowiaz, J., Ho, K.C., Ropelewski, C., Wary, J.,

LEETMA, A., REYNOLDS, R., JENNE, R. and JOSEPH, D., 1996, The NCEP/NCAR 40-years reanalysis project. *Bulletin of the American Meteorological Society*, **77**, pp. 437–471.

KATSAROS, K.B., FORDE, E.B., CHANG, P. and LIU, W.T., 2001, QuikScat's SeaWinds facilitates early identification of tropical depressions in 1999 hurricane season. *Geophysical Research Letters*, **28**, pp. 1043–1046.

KELLY, K.A. and CARUSO, M.J., 1990, A modified objective mapping technique for scatterometer wind data. *Journal of Geophysical Research*, **95**, pp. 13483–13496.

KELLY, K.A., DICKINSON, S. and YU, Z., 1999, NSCAT tropical wind stress maps: Implications for improving ocean modeling. *Journal of Geophysical Research*, **104**, pp. 11291–11310.

LIU, W.T., 2002, Progress in scatterometer application. *Journal of Oceanography*, **58**, pp. 121–136.

LIU, W.T., TANG, W. and POLITO, P.S., 1998, NASA scatterometer provides global ocean-surface wind fields with more structures than numerical weather prediction. *Geophysical Research Letters*, **25**, pp. 761–764.

LIU, W.T., XIE, X., POLITO, P.S., XIE, X.-P. and HASHIZUME, H., 2000, Atmospheric manifestation of Tropical Instability Wave observed by QuikSCAT and Tropical Rain Measuring Mission. *Geophysical Research Letters*, **27**, pp. 2545–2548.

MARINONE, S.G., PÁRES-SIERRA, A., CASTRO, R. and MASCARENHAS, S.G., 2004, Correction to 'Temporal and Spatial variation of the surface winds in the Gulf of California'. *Geophysical Research Letters*, **31**, L10305, doi: 10.1029/2004GL020064.

MILLIFF, R.F. and MORZEL, J., 2001, The global distribution of the time-average wind stress curl from NSCAT. *Journal of the Atmospheric Sciences*, **58**, pp. 109–131.

NIELSEN-GAMMON, J.W., 2001, The subtropical sea breeze. In *Proceedings of 9th AMS Conference on Mesoscale Processes*, Fort Lauderdale, FL, (30 July – 2 August 2001), American Meteorological Society: Boston, pp. 171–174.

PÁRES-SIERRA, A., MASCARENHAS, S.G., MARINONE, S.G. and CASTRO, R., 2003, Temporal and spatial variation of the surface winds in the Gulf of California. *Geophysical Research Letters*, **30**, 1312, doi: 10.1029/2002GL016716.

PEGION, P.J., BOURASSA, M.A., LEGLER, D.M. and O'BRIEN, J.J., 2000, Objectively derived daily 'winds' from satellite scatterometer data. *Monthly Weather Review*, **128**, pp. 3150–3168.

PICKETT, M.H., TANG, W., ROSENFELD, L.K. and WASH, C.H., 2003, QuikSCAT satellite comparisons with nearshore buoy wind data off the US West Coast. *Journal of Atmospheric and Oceanic Technology*, **20**, pp. 1869–1879.

QUIKSCAT 2001, *Remote Sensing Systems' Database for Satellite Microwave Data*, Available online at ftp://ftp.ssmi.com/qscat, (Accessed in 2004).

SCHLAX, M.G., CHELTON, D.B. and FREILICH, M.H., 2001, Sampling errors in wind fields constructed from single and tandem scatterometer datasets. *Journal of Atmospheric and Oceanic Technology*, **18**, pp. 1014–1036.

VERSCHELL, M.A., BOURASSA, M.A., WEISMAN, D.E. and O'BRIEN, J.J., 1999, Model validation of the NASA Scatterometer winds. *Journal of Geophysical Research*, **104**, pp. 11359–11374.

WENTZ, F., SMITH, D. and MEARS, C., 2001, Advanced algorithm for QuikSCAT and SeaWinds/AMSR. *Proceedings of IEEE 2001 International Geoscience and Remote Sensing Symposium*, 9–13 July, IEEE: Sydney, Australia, pp. 1079–1081.

YU, Z. and MOORE, D.W., 2000, Validating the NSCAT winds in the vicinity of the Pacific Intertropical Convergence Zone. *Geophysical Research Letters*, **27**, pp. 2121–2124.

ZAVALA-HIDALGO, J., YU, P., MOREY, S.L., BOURASSA, M. and O'BRIEN, J., 2003, A new interpolation method for high frequency forcing fields. In *Research Activities in Atmospheric and Ocean Modeling*, CAS/JSC Working Group on Numerical Experimentation, 2 pp.

ZENG, L. and LEVY, G., 1995, Space and time aliasing structure in monthly mean polar-orbiting satellite data. *Journal of Geophysical Research*, **100**, pp. 5133–5142.

Appendix: Stability correction of buoy data

Dependency of (RSS–buoy) wind speed residuals on atmospheric and oceanic conditions is examined. As shown in figure 13, the residuals for buoy 42020 are insensitive to both variations of the Ri number for the surface layer (positive values correspond to a stable stratification, and negative to an unstable) and the significant wave height (figure 13(*b*)). Similar results have been obtained for the other buoys (figures not presented). The solid lines in figure 13(*a*) indicate an expected relationship between a stratification surplus to the wind residuals and Ri for the buoy wind speed $5\,\mathrm{ms}^{-1}$ and $10\,\mathrm{ms}^{-1}$. Over most of the stability range, the stratification surplus is much smaller than observed (RSS–buoy) residuals, implying that this excess could be neglected. No systematic dependence of the residuals on the observed wind speed and the dominant wave frequency is found (figures not shown). When comparing the residual distributions for 00 UTC and 12 UTC, one can conclude that there is no significant difference between them.